

UNLOCKING THE POTENTIAL WITHOUT FRACKING – CO₂ INJECTION IN TIGHT SHALE OIL

Arthur U. Rognmo, Sunniva B. Fredriksen and Martin A. Fernø
Dept. of Physics and Technology, University of Bergen, Norway

This paper was prepared for presentation at the International Symposium of the Society of Core Analysts held in Vienna, Austria, 27 August – 1 September 2017

ABSTRACT

We present laboratory results on the feasibility of CO₂ injection to produce oil from tight shale oil without fracturing the formation. The hybrid process studied increased recoverable oil by an order of magnitude compared with fracking, and at the same time reduced the carbon footprint by associated CO₂ storage. Despite permeability values in the nano-Darcy range, we argue that CO₂-based EOR may successfully be implemented in shale oil formations. Core flooding injection tests showed a viscous dominated oil displacement for the initial oil recovery, changing into progressively more diffusional dominated over time. An average oil recovery of 34% of OOIP was obtained from CO₂ flooding experiments in reservoir core plugs. The experimental results demonstrate the potential to 1) increase oil recovery from shale oil compared with current production techniques, 2) reduce the need to rely solely on fracking to extract oil from tight shales, and 3) reduce the carbon footprint when combining oil recovery with CO₂-storage in unfractured shale core plugs.

INTRODUCTION

Worldwide energy demand is ever increasing and relies heavily on fossil fuels to provide energy security for the world in the years to come [1]. The last decade's geopolitical focus on decreasing the adverse environmental impacts caused by climate change illustrate the quandary faced by the world leaders; increase economic growth and human prosperity [2, 3] or decrease the concentration of greenhouse gasses in the atmosphere. Efforts to reduce CO₂ emissions must include the energy sector, as it is responsible for 60% of the global anthropogenic CO₂ emissions [4]. Sustainable supply of affordable and reliable energy urges a relentless focus on energy efficiency to ensure a prosperous future. Economic incentives from utilizing CO₂ after capture shifts the focus from pure Carbon Capture and Storage (CCS) to the Carbon Capture Utilization and Storage (CCUS) technology. A successful implementation of CCUS technologies reduces the carbon footprint from the energy sector and have the potential to achieve close to zero emissions [5]. Recent studies indicate the potential for safe long-term storage of CO₂ in cap rock shales or in tight gas shales [6]. In addition to the potential for pore space storage, shales (unlike e.g. sandstone) have a large storage potential due to their high sorption capacities.

Shift to Unconventional

As production rates from mature conventional oil fields decline, the petroleum industry is increasing its exploration of unconventional resources, such as shale oil [7-9]. Estimates of technically recoverable reserves in shale oil formations constitutes 10% of global oil resources. Recent significant US production volumes illustrate the large potential in these sources [10]. With recovery rates between 3-7% of oil originally in place (OOIP), and 58 billion barrels of technically recoverable reserves in the US alone, the potential for enhanced oil recovery (EOR) is enormous [10].

Oil recovery from secondary and tertiary production in conventional reservoirs is dominated by waterflooding [7]. However, the implementation of water injection for EOR in unconventional tight reservoirs is less efficient due to the ultra-low permeability associated with matrix composed of micro- and nano-pores [11]. Despite challenges related to the inherently ultra-low matrix permeability in shale oil formations, extracted volumes are viable due to a combination of water injection, horizontal drilling and hydraulic fracturing [12, 13]. However, rapidly declining production rates are frequently observed, resulting in short well operation times; the well economic shut-down time are considerable shorter compared to conventional reservoirs [14]. Water is extensively used in fracking operations as it is readily available at low cost [15]. It is, however, not without controversy and challenges; water is reported to reduce hydrocarbon flow back to the surface [14]. This is associated with additional costs as the flow back water needs to be treated for chemicals and other contaminants. In addition, due to the immense increase in water demand in combination with periods of drought in some parts of the US, water availability issues have emerged. Also, water flooding as a secondary recovery mechanism it is not expected to be feasible for ultra-tight formations, mainly due to low injectivity.

The utilization of CO₂ for EOR is widely proven in conventional reservoirs and has been commercially applied for more than 40 years in the US. Favorable CO₂ properties at reservoir conditions promotes oil recovery, primarily by oil phase swelling, viscosity alteration, interfacial tension reduction and higher degree of crude oil miscibility, compared to other gasses. These conditions are also considered to be present in tight shale oil formations [16], but a comprehensive understanding of its underlying mechanisms is needed. EOR is a relatively new concept in tight oil reservoirs. To date, the reported experimental studies of EOR in tight shale oil focuses on utilizing fractures for contacting, displacing and transporting oil [17-19]. The presumption is that due to the inherently ultra-low permeabilities associated with these formations, conventional core analysis with pressure driven viscous oil displacement and transport is not possible. Hence, recovery relies on the concentration driven oil displacement from molecular diffusion in the fractures to the oil saturated matrix.

This paper presents results from a comprehensive experimental study on CO₂-EOR in reservoir shale oil core plugs, where a high differential pressure was applied. The accelerated effect of, and increased oil recovery from, viscous oil displacement was studied without fracking the formation. Results demonstrate the feasibility of utilizing

CO₂ flooding as a recovery mechanism in shale oil formations. Effects on oil recovery and rate of recovery from varying system length, pressure, time and oil composition were investigated.

MATERIALS AND METHODS

Core Material

Five cylindrical reservoir core plugs with 1” and 1.5” diameters and length of 1.5-2.5” were used, see Table 1. All core plugs were from a producing shale oil formation in the US, with different states of preservation: cores 1, 2 and 3 were considered restored-state cores (subjected to CO₂-injection tests and re-saturated with crude oil); core 4 and 5 were considered native-state upon arrival. All cores were received at ambient temperature and pressure and rock structure of each core was imaged with a medical X-ray computed tomography (CT) scanner located at Haukeland University Hospital. Variations in permeability (0.12 to 2.36 μ D) and porosity (4.5 to 9.3%) were expected due to different extraction depths. The oil phase saturating the pore space for the different experiments was either n-Decane (mineral oil: MO) or a light North Sea crude oil (CO, American Petroleum Institute gravity 38) as listed in **Table 2**.

Table 1 – Characteristics of reservoir shale oil core plugs

Core ID	Length [cm] $\pm 2E-3$ [cm]	Diameter [cm] $\pm 2E-3$ [cm]	Porosity [%]	Permeability [μ D]
Core 1	3.798	3.796	4.8	0.12
Core 2	3.923	3.796	4.5	0.74
Core 3	2.450	3.820	7.0	1.70
Core 4	5.150	2.520	9.3	1.85
Core 5	5.115	2.540	7.0	2.36

Oil Saturation Procedure

Re-saturating the core plugs with oil after each CO₂ flooding was necessary to perform repeated tests for increased statistical significance. Reproducible initial oil saturations were achieved prior to each experiment by submerging the core plugs completely in the selected oil phase (mineral oil or crude oil) in a high-pressure stainless steel accumulator. The saturation process lasted for four days, with a saturating pressure of 10 MPa for mineral oil and 20 MPa for crude oil. Based on weight differences before and after saturation, along with density of the oil, the OOIP was calculated.

Table 2: Fluid properties

Fluid	Composition	Density [g/cm ³]	Viscosity [cP]	Conditions		Fluid State
				Temperature [°C]	Pressure [bar]	
n- Decane	C ₁₀ H ₂₂	0.727	0.848	25.0	1.0	Liquid
		0.734	0.952	25.0	100.0	Liquid
		0.709	0.610	60.0	100.0	Liquid
Crude oil	53 wt. % saturated HCs 35 wt. % aromatics 12 wt. % resins 0.90 wt. % asphaltenes	0.849	14.500	20.0	1.0	Liquid
		0.829	-	60.0	1.0	Liquid
Carbon dioxide	> 99.999 % CO ₂	0.876	0.086	25.0	150.0	liquid
		0.927	0.098	25.0	220.0	liquid
		0.604	0.046	60.0	150.0	supercritical
		0.752	0.064	60.0	220.0	supercritical

Experimental Setup and Procedure for CO₂ Injection

The core plugs were installed in a horizontal biaxial Hassler type core holder (*CoreLab Hassler Type Core Holder*) with a Buna-N rubber sleeve, inside a heating cabinet. A net radial confining pressure of 6.0 MPa (870 psia) was applied during the pressurization period and increased to 9.0 MPa (1305 psia) above inlet pressure during the CO₂ flooding tests. A total of 14 injection tests on crude oil saturated core plugs were performed at 60°C (±0.5°C), with a constant differential pressure drop of 7.0 MPa (1015 psia) and an inlet line pressure of 22.0 MPa (3190 psia). Hence, the volumetric injection rate varied depending on the fluid flow capacity of the particular core plug and oil was displaced from inlet towards outlet. Four injection tests were performed using n-Decane saturated core plugs with a lower inlet pore pressures (17.0 MPa – 2465 psia) and at 25°C, other properties being equal. The experimental setup is shown in Figure 1. The effluent fluids were cooled by a water based heat exchanger located downstream the back pressure regulator (*Equilibar HC276-5*), measured at ambient conditions (20°C and 1 bar). A camera and an image software with a time-lapse function was used to calculate oil recovery as a function of pore volumes (PV) CO₂ injected. Permeabilities were calculated from parameters obtained at steady state conditions, i.e. all recoverable oil was produced. It is therefore reasonable to assume CO₂ to be the only flowing phase in the core plugs, and by correcting for viscosity and density differences across the core, the end point effective permeability for CO₂ was obtained. The cores were not wrapped in an impermeable barrier (like Aluminum- or Nickel-foil), a common procedure to prevent CO₂ from permeating the core sleeve. Access to a new methodology to explicit track CO₂ with positron emission tomography [20], revealed that the injected CO₂ bypassed the

core, even with a net confinement pressure of 9MPa, when a foil was used. We speculate that small folds and creases in the foil caused minute flow paths for the CO₂ – preferred over the pore space of the tight shale oil samples. All reported injection tests are therefore performed without foil in this work.

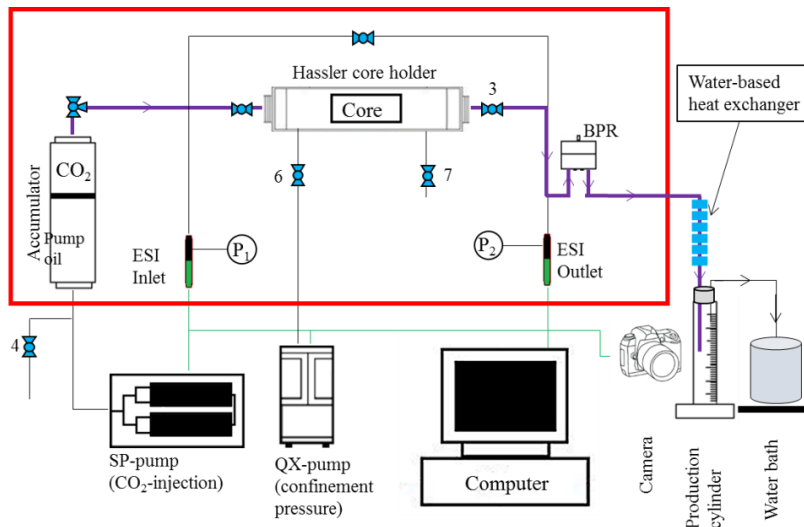


Figure 1: Schematic illustration of the experimental setup used for EOR by supercritical CO₂-injection in tight shale oil reservoir core plugs. Purple lines illustrate injection and production flow paths; arrows indicate flow direction. Green lines illustrate digital information cables from pressure transducers, pumps and camera; connected to a computer for processing and analysis. Black lines illustrate remaining tubing. The heating cabinet is represented by the thick red rectangle.

RESULTS AND DISCUSSION

The main message communicated in this paper is that CO₂-EOR effectively displaced oil during differential pressure driven fluid flow in ultra-tight liquid shales (see Figure 2). Fractures were not introduced before or during the flooding tests, and oil was displaced from the injector (inlet) to the producer (outlet), driven by the pressure gradient over the core. Oil recoveries for all experiments are plotted as recovery factor (R_f) in % of OOIP as a function of PV CO₂ injected, where the starting point was set as the time where the first drop of oil was recorded. Based on repeated CO₂ end-point effective permeability measurements fluid flow potential in the core plugs did not change after each successive CO₂ injection process. Superficial velocities (obtained from permeability measurements at endpoint effective CO₂ permeability) ranged from 0.2 – 2.1 ft/day for the five cores.

CO₂-EOR in Tight Shale Oil

Recovery profiles for four CO₂ floods in crude oil saturated core plugs are shown in Figure 2. The slopes of the recovery profiles indicate the recovery rates, where the highest rate is observed in the early stages of the CO₂ flooding with a progressively decreasing rate of recovery over time. This behavior indicates that the oil displacement became more dominated by molecular diffusion (the spontaneous mixing of miscible fluids due to random motion of molecules down its concentration gradient) over time.

The recovery profiles suggest poor sweep efficiency and early CO₂ breakthrough from CO₂ channeling. The CO₂ was not first-contact miscible with the crude oil, hence, a longer transition zone for development of multi-contact miscibility is needed [21].

Table 3: Key parameters during liquid and supercritical CO₂ injections. Oil saturating the pore space is either n-Decane mineral oil (MO) or a light North Sea crude oil (CO).

Core ID	Injection ID	Oil phase	Temperature [°C]	Final recovery factor [%]	OOIP [mL]	Final average recovery factor [%]
Core 1	A	CO	60	98.3	1.63	52.7
Core 1	B	CO	60	25.1	1.59	
Core 1	C	CO	60	34.7	1.87	
Core 2	A	CO	60	22.7	1.54	28.1
Core 2	B	CO	60	29.1	1.54	
Core 2	C	CO	60	32.4	1.54	
Core 3	A	CO	60	26.8	1.68	26.1
Core 3	B	CO	60	25.4	1.97	
Core 4	A	CO	60	31.6	1.42	19.8
Core 4	B	CO	60	7.1	1.41	
Core 4	C	CO	60	20.7	1.21	
Core 5	A	CO	60	28.3	1.41	28.3
Large	A	CO	60	55.3	5.07	55.3
Core 1	A	MO	60	60.0	1.58	68.0
Core 3	A	MO	25	73.2	1.84	
Core 3	B	MO	25	81.0	1.79	
Core 3	C	MO	60	57.7	1.73	

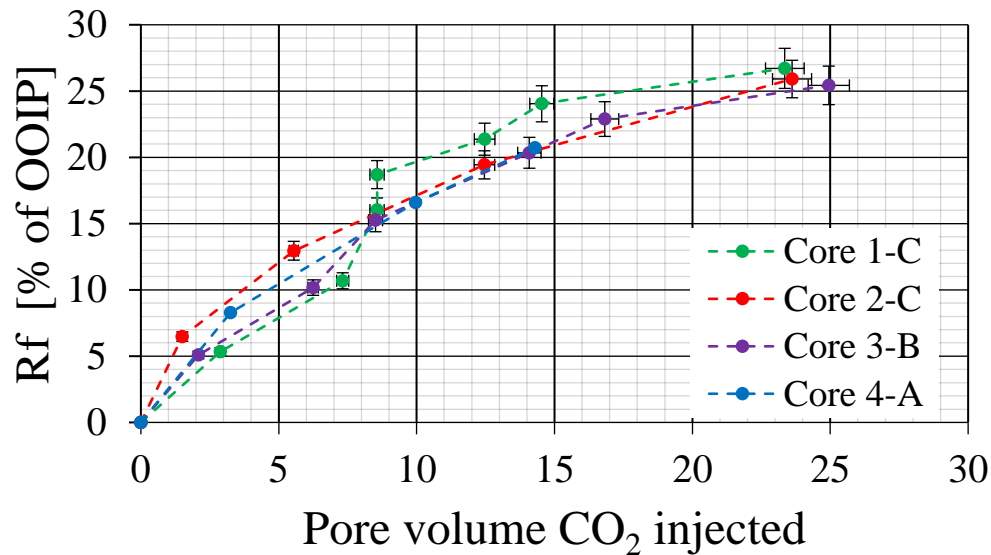


Figure 2: Recovery factor (% of OOIP) vs. time (pore volumes CO₂ injected) for four CO₂-EOR flooding tests in tight shale oil reservoir core plugs, saturated with crude oil. Filled circles indicate measured values. The main observation is that conventional CO₂-EOR can extract fluids from, and flow through, unfractured tight shales, despite nano-Darcy permeability range.

Effect of Oil Composition

To investigate the effects of first-contact miscible displacements the saturation fluid was changed to mineral oil. This enabled quantitative evaluation of the displacement process and recovery rate. A one-component mineral oil was used (n-Decane) for the oil phase and four first-contact miscible CO₂ flooding tests were performed, at 60°C and 25°C. The oil recovery profiles showed an improvement in both final recovery and rate of recovery compared to multi-contact miscible displacements (cf. Figure 3).

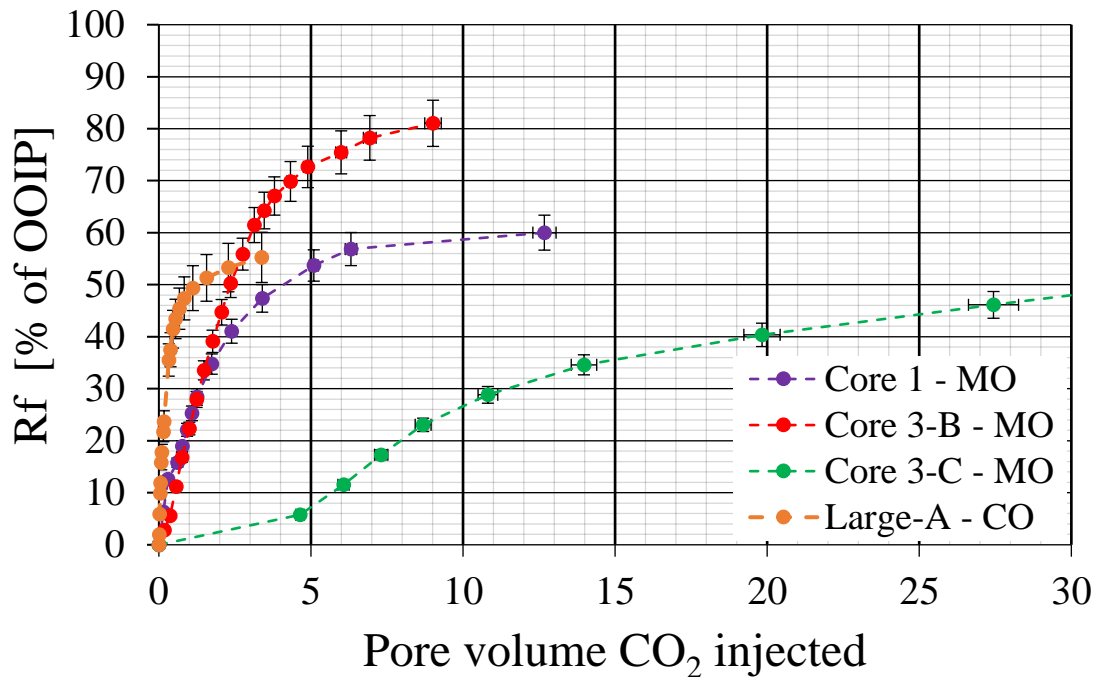


Figure 3: Recovery factor (% of OOIP) vs. time (pore volumes CO₂ injected) for four first-contact miscible CO₂-EOR flooding tests in tight shale oil reservoir core plugs. Core 1-A-MO and 3-C-MO are performed at 60°C and Core 3-A-MO and 3-B-MO are performed at 25°C. The points are measured values and a linear production as function of CO₂ injected from one point to the next is assumed. The graph display fast recovery in the beginning and gradually slower rate of recovery. Note the x-axis has been cropped at 30 PVs injected, final recovery Core 3-C-MO is 57.7 % of OOIP (± 3.2 % of OOIP) at 41.5 PVs (± 1.2 PVs) injected.

Effect of System Size

A larger system (see Table 3 for key properties) was obtained by placing three cores in succession to study the impact of system size on displacement efficiency. Increased length was expected to promote the development of miscibility between injected CO₂ and crude oil by increasing the transition zone length [21]. Two flooding test were performed at 60°C and 7.0 MPa (1015 psia) differential pressure. One flooding test was performed for 3.6 days, yielding a CO₂ injection of 0.18 PVs. Visual inspection of the three cores

showed development of viscous fingers and CO₂ flow influenced by gravitational segregation (cf. Figure 4) at the inlet-end core, whereas no indications of oil displacement was observed for the middle core and the outlet-end core. Due to the high mobility ratio and density difference, CO₂ perturbations occur and override parts of the crude oil phase, causing front instabilities. The second test ran for 8 days, injecting a total of 3.7 PVs CO₂. For the first 5 days, 0.02-0.06 PV CO₂ was injected with low injection rate, assumingly related to the time needed for miscibility to be developed. The viscous driving force was reduced, compared with CO₂ injections in single cores, by a factor of three due to lower pressure drop per unit length. The increased length resulted in a slower front propagation, and, therefore, increased CO₂ exposure to crude oil, favorable for miscibility to develop.

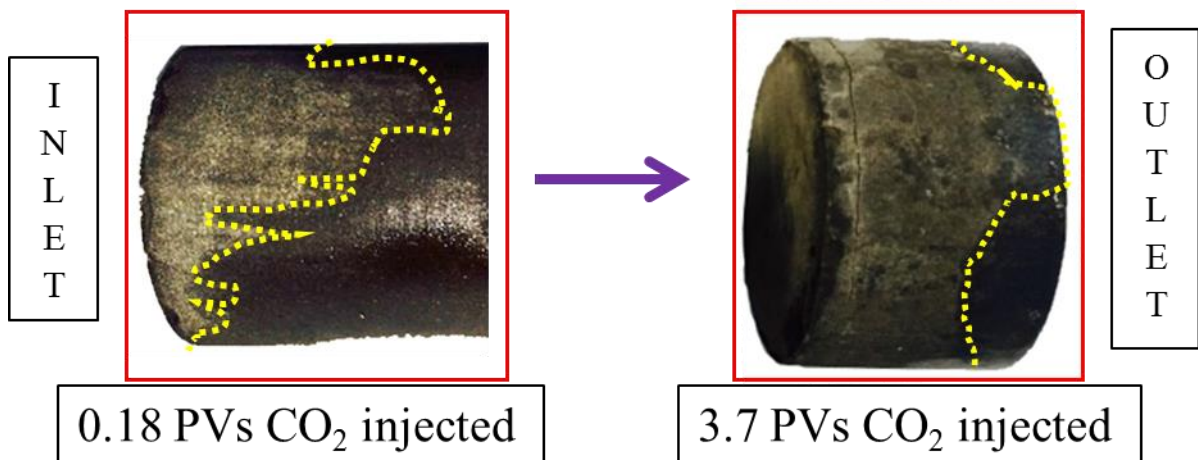


Figure 4: Left picture (after 0.18 PVs CO₂ injected) in large system shows the swept areas (grey) where CO₂ has displaced crude oil. The jagged front (highlighted with dotted yellow line) suggests viscous fingering of the CO₂ through the crude oil saturated inlet core. The arrow indicates the direction of flow (the pressure gradient). Right picture (after 3.7 PV CO₂ injected) shows visual observations of swept area (grey) in the outlet core (inlet and middle core completely swept), and display a more homogeneous front development.

Dispersions (and especially diffusion) are likely to dampen the adverse effects of viscous fingers and may explain the shape of the recovery curves obtained; higher rate of recovery early in the injection phase and progressively lower rate of recovery with time. (see Figure 5). Viscous displacement was assumed to dominate in the early stages of injection, whereas oil was recovered by diffusional driven displacement at later stages. Visual observations of the color of produced oil corroborated this, because the heavier components, with relatively lower diffusional coefficients, were produced at the late stage, in agreement with [22]. On larger scales diffusion is perceived as a slower process compared to capillary and viscous driven displacement processes, however it is spontaneous, causing it to be continuous and ubiquitous [6].

The dynamic production profile (see Figure 5) indicates that CO₂ breakthrough occurred after approximately 0.5 PV CO₂ injected (Rf @ CO₂ breakthrough: 41.5% of OOIP). Additional recovery is assumed to mainly occur from the developed multi-contact miscibility caused by molecular diffusion, and a final oil recovery factor yielded 55.0% ($\pm 9.2\%$) of OOIP after a total of 3.7 (± 0.2) PV CO₂ injected, suggesting high degree of miscibility.

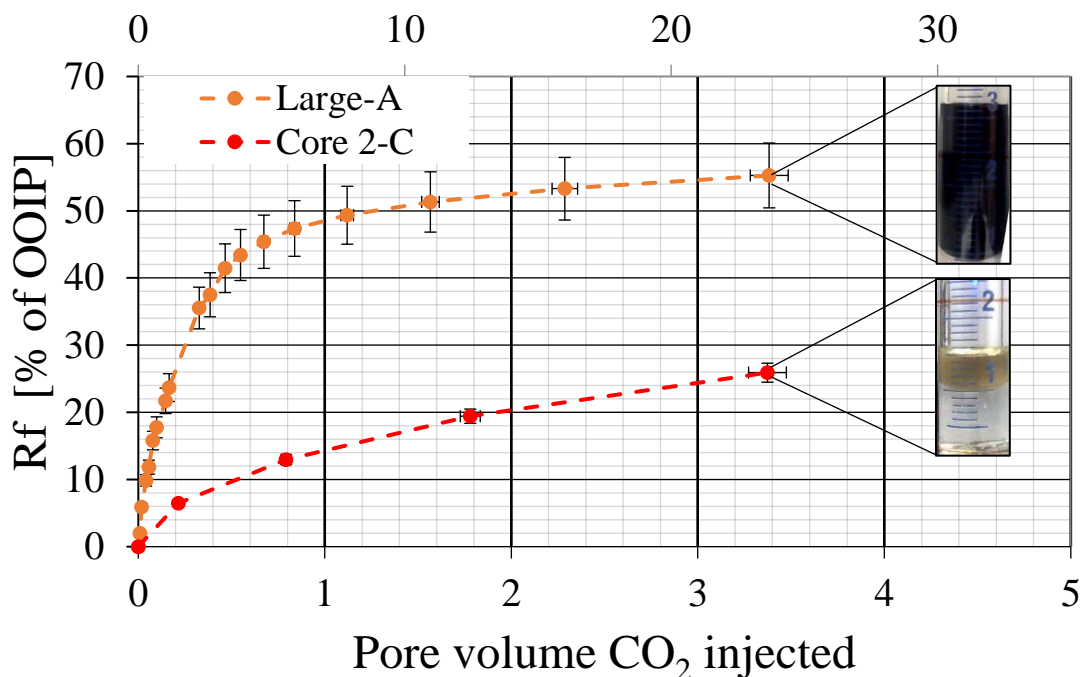


Figure 5: Oil recovery (%OOIP) vs. time (pore volume CO₂ injected) for increased system size (large) and single core plug (core 2). The points are measured values and a linear production as function of CO₂ injected from one point to the next is assumed. The large system size graph display fast recovery in the beginning and gradually slower rate of recovery with a recovery factor yielded 55.0% ($\pm 9.2\%$) of OOIP after a total of 3.7 (± 0.2) PV CO₂ injected. The single core plug system (Core 2-C) display a slower rate of recovery and the final recovery is lower (23.6 % of OOIP). The produced oil (inset) shows a distinct difference in oil composition further corroborating the importance of system size.

Impact of Time on Oil Recovery

The relationship between PVs of CO₂ injected, injection time and final recovery was calculated for the two main parameters investigated in this work: oil phase (degree of miscibility) and system length. The arithmetic average of oil recovery for three groups (mineral oil, crude oil and large) was used to increase statistical significance in each group (see Figure 6. Area represents the final oil recovery, and indicates a tradeoff between injection rate (volume needed) and flooding time (time needed). Comparison between first-contact miscible displacement (orange circle: Rf= 68% of OOIP) and multi-contact miscible displacement (blue circle: 33.7% of OOIP) show that both the injection

time of CO₂ exposure (hours) and volume of CO₂ injected is considerable lower for systems with higher degree of miscibility. Due to the favorable displacement, the final oil recovery was higher by a factor of two, emphasizing the beneficial impact of diffusion as previously mentioned. Increased system size had a strong effect on the final oil recovery as a function of pore volumes injected. The final recovery was comparable with first-contact miscible displacement at lower pore volumes injected, the tradeoff being the increased time for a high degree of miscibility to develop.

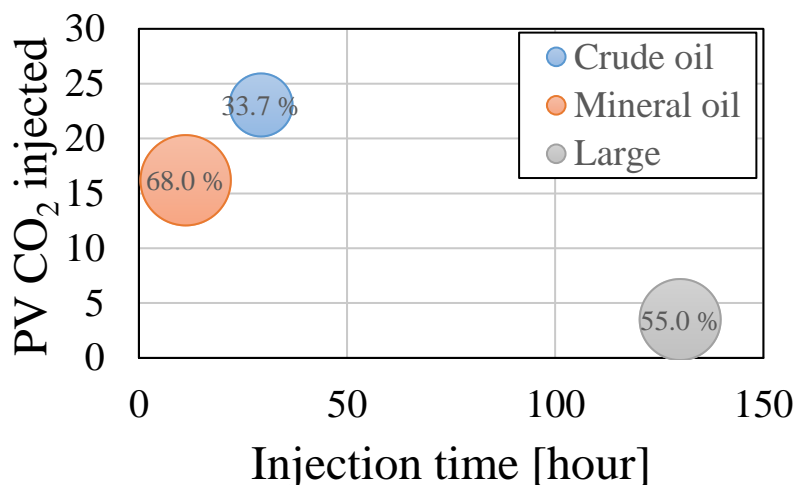


Figure 6: Arithmetic average values of pore volumes CO₂ injected, time of exposure and final oil recovery for seventeen CO₂-EOR flooding tests, performed at reservoir conditions. Time is longer and volumes of CO₂ needed is higher to recover crude oil from single cores, compared to mineral oil recovery. By increasing the time of contact between CO₂ and crude oil, the recovery factor increases and the volumes needed for EOR decreases.

Because some of the miscibility process is assumed to include exchange of particles perpendicular to the direction of flow (by diffusion) and this is time dependent, it seems reasonable that the oil recovery increases due to larger volumetric sweep efficiency as the contacted time increases. However, the surface area of contact is equally important and the stronger effect observed by the cores permeability seems to have larger impact on the rate of developed miscibility and the degree of miscibility.

CONCLUSIONS

In this paper we show that conventional CO₂-EOR can be implemented on ultra tight shale oil core plugs, reaching oil recovery fractions as high as 98.3% of OOIP; without introducing fractures to the system.

An average oil recovery factor of 33.7% of OOIP was achieved for thirteen crude oil saturated core plugs under multi-contact miscible conditions. An average oil recovery factor of 68.0% of OOIP for four mineral oil saturated core plugs under first-contact miscible conditions.

Rate of oil recovery and final oil recoveries are shown to have a positive correlation with system size and CO₂ exposure time.

ACKNOWLEDGEMENTS

The authors would like to thank the Research Council of Norway and Statoil for financial support and contributions.

REFERENCES

1. Tour, J.M., C. Kittrell, and V.L. Colvin, Green carbon as a bridge to renewable energy. *Nature Materials*, 2010. **9**(11): p. 871-874.
2. Chu, S. and A. Majumdar, Opportunities and challenges for a sustainable energy future. *Nature*, 2012. **488**(7411): p. 294-303.
3. Aldy, J.E., et al., Designing Climate Mitigation Policy. *J.I of Economic Literature*, 2010. **48**(4): p. 903-34.
4. IEA, CO₂ Emissions from Fuel Combustion. 2015: p. 548.
5. Riahi, K., et al., Technological learning for carbon capture and sequestration technologies. *Energy Economics*, 2004. **26**(4): p. 539-564.
6. Busch, A., et al., Carbon dioxide storage potential of shales. *International Journal of Greenhouse Gas Control*, 2008. **2**(3): p. 297-308.
7. Alvarez, J.M. and R.P. Sawatzky, Waterflooding: Same Old, Same Old? 2013, *Society of Petroleum Engineers*.
8. Etherington, J.R. and J.E. Ritter, The 2007 SPE/WPC/AAPG/SPEE Petroleum Resources Management System (PRMS). 2008.
9. Alvarado, V. and E. Manrique, Enhanced Oil Recovery: An Update Review. *Energies*, 2010. **3**(9): p. 1529.
10. EIA, Technically Recoverable Shale Oil and Shale Gas Resources: An Assessment of 137 Shale Formations in 41 Countries Outside the United States. 2013: p. 730.
11. Kuila, U., I. Berend, and M. Prasad, Specific surface area and pore-size distribution in clays and shales (vol 61, pg 341, 2013). *Geophysical Prospecting*, 2014. **62**(1): p.196
12. Wang, W., et al., A mathematical model considering complex fractures and fractal flow for pressure transient analysis of fractured horizontal wells in unconventional reservoirs. *Journal of Natural Gas Science and Engineering*, 2015. **23**: p. 139-147.
13. Sheng, J.J., Enhanced oil recovery in shale reservoirs by gas injection. *Journal of Natural Gas Science and Engineering*, 2015. **22**: p. 252-259.
14. Pei, P., et al., Shale gas reservoir treatment by a CO₂-based technology. *Journal of Natural Gas Science and Engineering*, 2015. **26**: p. 1595-1606.
15. Middleton, R.S., et al., Shale gas and non-aqueous fracturing fluids: Opportunities and challenges for supercritical CO₂. *Applied Energy*, 2015. **147**: p. 500-509.
16. Jarrell, P.M. and R.T. Jones, Practical aspects of CO₂ flooding. Henry L. Doherty series. Vol. vol. 22. 2002, Richardson, Tex: Henry L. Doherty Memorial Fund of AIME, *Society of Petroleum Engineers*.
17. Tovar, F.D., et al., Experimental Investigation of Enhanced Recovery in Unconventional Liquid Reservoirs using CO₂: A Look Ahead to the Future of Unconventional EOR. 2014, *Society of Petroleum Engineers*.
18. Gamadi, T.D., et al., An Experimental Study of Cyclic CO₂ Injection to Improve Shale Oil Recovery. 2014, *Society of Petroleum Engineers*.

19. Vega, B., et al., Experimental Investigation of Oil Recovery From Siliceous Shale by Miscible CO₂ Injection. 2010, *Society of Petroleum Engineers*.
20. Fernø, M. A., Hauge, L. P., Uno Rognmo, A., Gauteplass, J. & Graue, A. 2015. Flow visualization of CO₂ in tight shale formations at reservoir conditions. *Geophysical Research Letters*, 42, 7414-7419.
21. Lake, L.W., et al., Fundamentals of Enhanced Oil Recovery. 2014, 222 Palisades Creek Dr, Richardson, TX 75080, USA: *SPE*.
22. Darvish, G.R., et al., Reservoir Conditions Laboratory Experiments of CO₂ Injection into Fractured Cores. 2006, *Society of Petroleum Engineers*.